KFUPM
Journal of Undergraduate Research International

Diamond Open Access 89

Article Material Science and Engineering/Physics

# Antenna Design for Aircraft Situational Awareness: Coverage of ADS-B/TCAS and UHF SATCOM Frequencies

Taqi Abdulkhaleg Albaiyat and Bazilah Binti Baharom*

Cite https://doi.org/10.64589/juri/215033

**Submitted:** September 14, 2025 **Revised:** November 17, 2025 **Accepted:** December 02, 2025

**ABSTRACT**

This paper presents the design and simulation of a broadband blade antenna for aeronautical and astronautical communication systems, including the Traffic Collision Avoidance System (TCAS), Automatic Dependent Surveillance–Broadcast (ADS-B), and UHF satellite communications (SATCOM). Using CST Studio Suite, a compact blade-type antenna was modeled to operate from 400 MHz to 1.1 GHz, covering both SATCOM (approximately 400–500 MHz) and ADS-B/TCAS (1030–1090 MHz). Performance parameters, such as reflection coefficient, surface current distribution, far-field radiation pattern, gain, and efficiency, were analyzed at multiple frequencies. The results indicate broadband impedance matching, as evidenced by an $S_{11}$ value below −10 dBi, along with consistent gain ranging from 7.363 dBi to 8.282 dBi throughout the operational frequency band. Compared to conventional aircraft platforms with multiple narrowband antennas, a single wideband blade antenna offers distinct benefits such as reduced aerodynamic drag, lower weight and cabling, simplified certification and maintenance, and improved system integration with reduced electromagnetic interference. By combining multiple services into one compact structure, the proposed design provides an integrated, cost-effective, and aerodynamically efficient solution for modern aircraft and UAV platforms, enhancing the reliability and communication performance across critical missions. We expect the proposed preliminary design blade antenna can contribute to future aircraft technologies.

**Keywords:** blade antenna, automatic dependent surveillance broadcast, traffic collision avoidance system, ultra-high frequency satellite communication, aeronautical communications, airborne systems

## 1. INTRODUCTION

The aviation and aerospace industries continue to demand high-performance antenna systems capable of supporting various communication and navigation functions within compact and aerodynamically efficient form factors. Among these, the Traffic Collision Avoidance System (TCAS), Automatic Dependent Surveillance–Broadcast (ADS-B), and UHF Satellite Communications (SATCOM) are essential for maintaining flight safety, aircraft coordination, and reliable long-range communications [1,2]. Figure 1 shows the distribution of multiple communication and navigation antennas on a Boeing 787 aircraft, where each antenna serves a specific function such as TCAS, ADS-B, and other systems, illustrating the complexity and aerodynamic impact of using multiple narrowband antennas and suggesting the advantages of one wideband antenna for reducing drag, weight, and system-integration challenges.

Conventional aircraft platforms often rely on multiple narrowband antennas to cover specific frequency ranges. While effective, this approach, increases system complexity, weight, and cost while reducing aerodynamic performance. By contrast, blade antennas, a subclass of monopole structures, balance mechanical robustness, aerodynamic integration, and reliable electrical performance across operational bands [3–5]. Recent research emphasizes their potential for integration into aircraft-fuselage conformal surfaces [6,7].

Various blade-antenna configurations have been proposed for specific communication applications. Pascawatia et al. [8] developed a blade antenna for 2.4 GHz rocket telemetry; Belen et al. [9] explored UHF-oriented blade antennas for vehicular and aeronautical systems; Sairam et al. [10] introduced broadband blade antennas for airborne platforms; and Saaquib et al. [11] incorporated air-core coils and horizontal notches to improve impedance bandwidth and matching. Silva et al. [12] embedded blade antennas in low-cost dielectric substrates to reduce costs while maintaining performance stability.

Figure 2 shows the communication architecture of a remotely piloted aircraft. The uplink commands and downlink status updates are transmitted through direct ground links or via a SATCOM relay, alongside. An ATC communication link facilitates flight coordination. This illustrates the objective of this study: to design a wideband blade antenna that operates across the range of UHF SATCOM and ADS-B/TCAS frequencies, integrating these critical links into a single-antenna structure. By consolidating multiple communication services into one

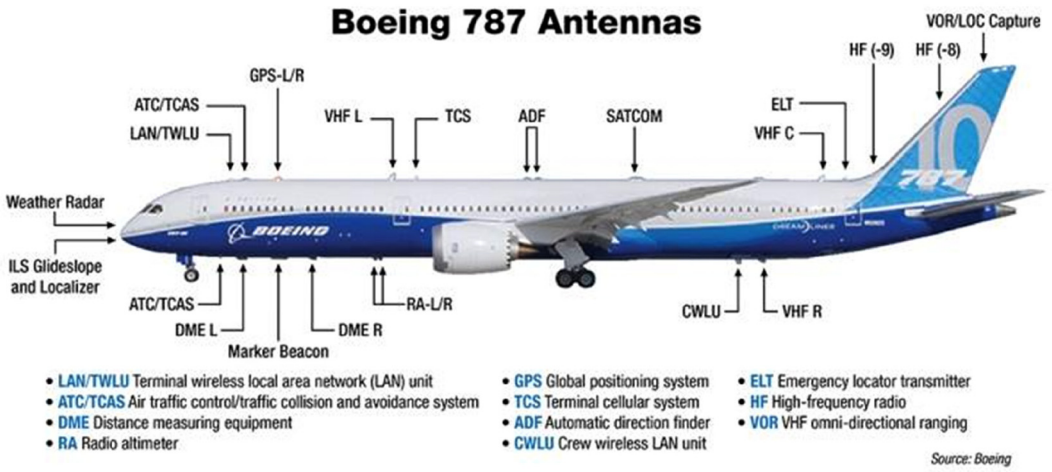


**Figure 1.** Communication, navigation, and surveillance antennas on the Boeing 787 aircraft

antenna, the design reduces reliance on separate narrowband antennas, improving aerodynamic efficiency and simplifying system integration for both manned/unmanned aircraft platforms.

However, designing a single compact-blade antenna that seamlessly covers 400 MHz to 1.1 GHz (crucial for UHF SATCOM and ADS-B/TCAS) remains challenging. Therefore, this study aims to design and analyze wideband blade antenna using CST Studio Suite, and emphasizes on impedance stability, gain consistency, radiation efficiency, and directional behavior across the targeted spectrum [13–15].

## 2. ANTENNA DESIGN

This section details the antenna design and choice of substrate material. The proposed blade-type antenna structure is mounted on a rectangular ground plane optimized to achieve wideband coverage suitable for aeronautical and astronautical communication applications. Figure 3 shows the geometries of the preliminary and proposed designs. The ground plane is 400 × 850 ×10 mm in size, providing a stable platform for the radiating element and acting as a reflector to enhance performance. The blade radiator has a total height of approximately 490 mm and thickness of 10 mm, and it is tilted 45° relative to the ground plane. This tilt improves radiation efficiency and reduces impedance mismatch, which is common challenge in wideband monopole configurations. An SMA feed pin excites the radiator, ensuring proper coupling with the ground plane to support broadband operation across the targeted frequency range of 0.4–1.1 GHz.

The blade antenna was modeled using a perfect electric conductor (PEC) material for the metallic structure, which is used in aerospace antenna design owing to its excellent electrical and mechanical characteristics. The PEC plate with a thickness of 10-mm ensures robust structural integrity under aerodynamic loading while minimizing ohmic losses. The initial shape and dimensions of the preliminary blade antenna were selected based on insights from previous studies on broadband monopole and blade antennas [8,12] , which revealed that radiator geometry and feed positioning are crucial for achieving multiband operation. Building on this foundation, the design was further refined and optimized to meet the research objectives. The selected

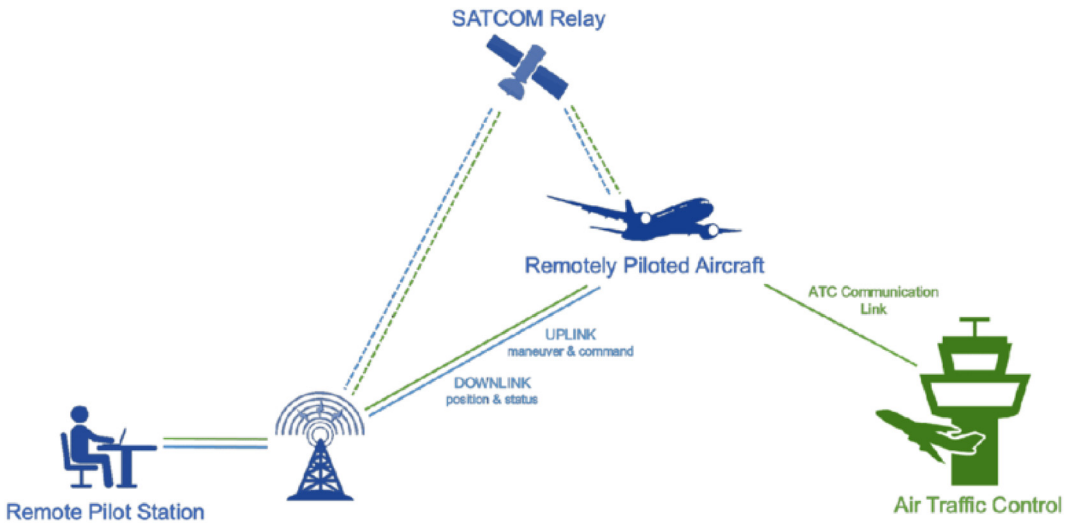


**Figure 2.** Communication links of a remotely piloted aircraft using a SATCOM relay, ground station, and air-traffic control

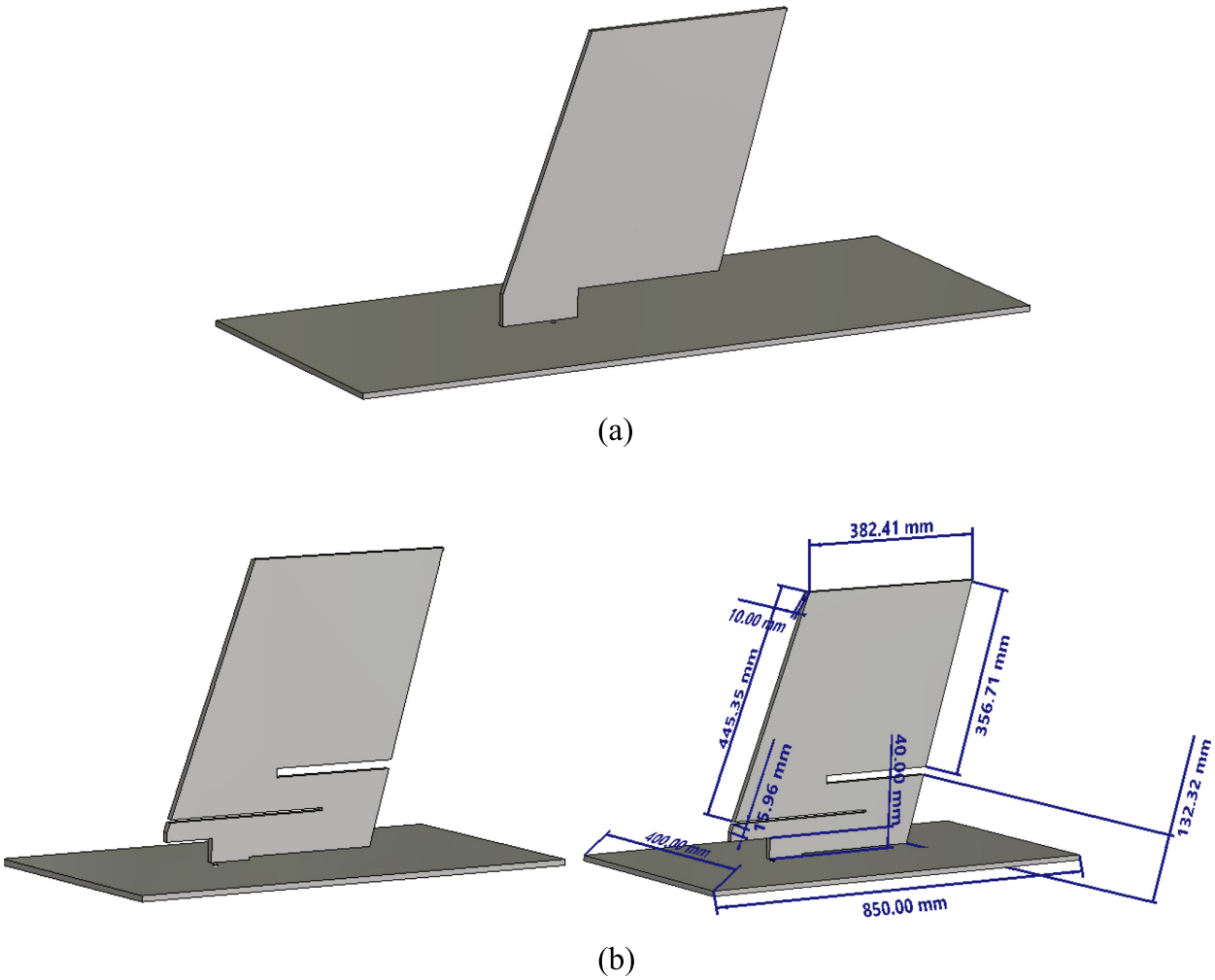


**Figure 3.** Configuration of blade antenna design: (a) preliminary design and (b) optimized blade antenna design: (left) clean version and (right) with dimensions

configuration enables the antenna to cover the UHF SATCOM (400–500 MHz) and ADS-B/TCAS (1030–1090 MHz) bands.

**2.1. Optimization Method.** The preliminary antenna geometry, which was designed manually based on a detailed review of existing broadband blade antenna designs reported in the literature [8–12]. To further enhance the antenna's performance, a parametric sweep optimization performed using CST Studio Suite. The optimization process began with the basic geometry shown in Figure 3 (a). Successive refinements were then introduced based on the observed electromagnetic behavior. First, a horizontal slit was added near the upper part of the blade at the back to broaden the impedance bandwidth. Next, the slit position and length were adjusted toward the blade's upper back corner to improve matching across the target frequency bands. To enhance the multiband performance, a two-stage parametric sweep was executed in which the slit length was varied from 20 to 80 mm in 5 mm increments, while the slit width was adjusted between 2 and 6 mm. Performance was evaluated using the reflection coefficient ($S_{11}$) <–10 dB, voltage standing wave ratio (VSWR) <2, and gain stability at 0.43, 0.5, 1.03, and 1.09 GHz.

To better understand the effect of each modification on the affected performance, the surface current distributions were analyzed at every iteration. These current maps revealed regions of strong current concentration around the feed and ground-plane junctions. Based on these observations, an additional ground-plane cutout surrounding the SMA connector region was introduced to reduce local current crowding and improve the overall impedance characteristics.

Finally, a second slit was added and optimized in the lower front section of the blade, to complete the design evolution. This final configuration Figure 3 (b) provides the most favorable combination of wideband impedance matching, stable radiation behavior, and peak gain performance. The optimization of the blade antenna geometry was through a structured parametric sweep analysis using CST Studio Suite. The optimized geometry provided the widest impedance bandwidth and maintained a peak gain exceeding 7.3 dBi across all required frequency bands.

**2.2. Material, Feed Selection, and Simulation Setup Considerations.** The antenna is installed using an SMA/N-type connector and bonded to the fuselage ground plane,

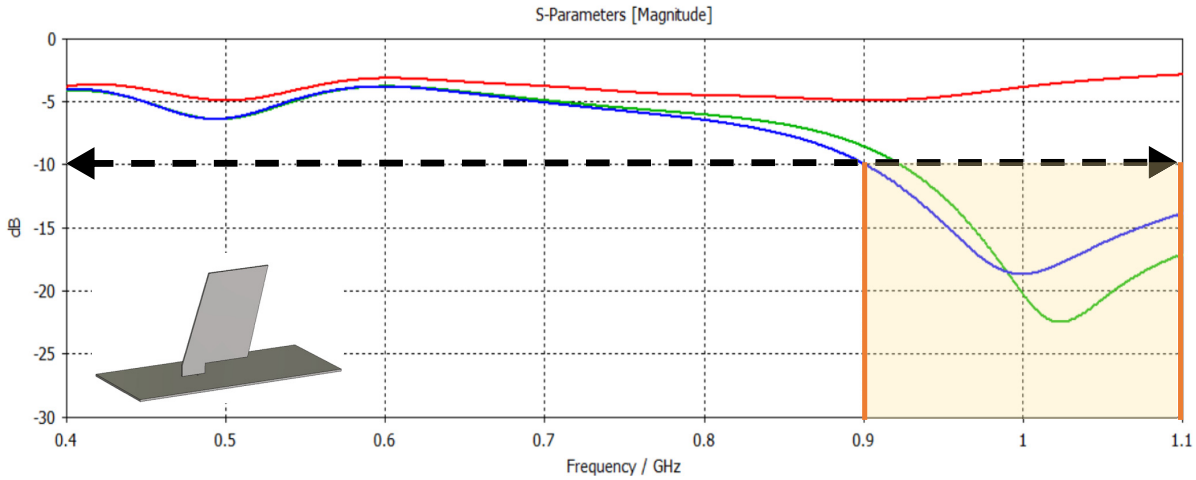


(a)

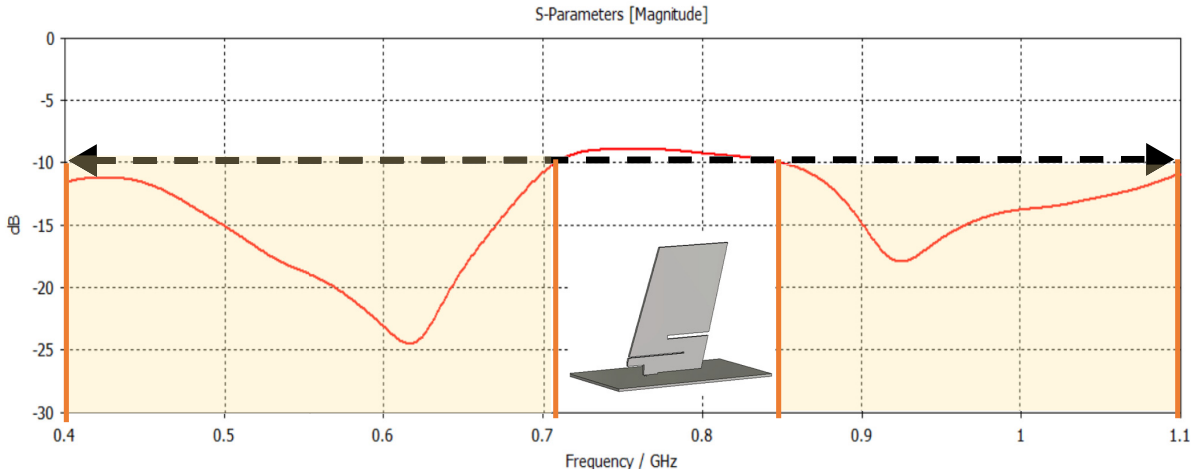


(b)

**Figure 4.** Reflection coefficient ($S_{11}$) versus frequency of the proposed blade antenna: (a) preliminary blade antenna and (b) optimized blade antenna

following the same concept used in[8–12]. In future simulations, a thin dielectric radome may be included to protect the antenna assembly from environmental factors such as rain, lightning, and aerodynamic forces that could impact structural integrity.

## 3. PERFORMANCE EVALUATION

Simulations were performed in CST Studio Suite using open boundary conditions to replicate the free-space performance. Key metrics such as $S_{11}$, surface current distribution, far-field radiation patterns, gain, and VSWR were evaluated. Representative frequencies at 0.43 GHz, 0.50 GHz, 1.03 GHz, and 1.09 GHz were selected for detailed analysis, corresponding to the operational ranges of SATCOM and ADS-B/TCAS. This systematic approach ensures that the antenna meets the broadband performance requirements while maintaining stable gain and radiation efficiency across multiple bands.

Figure 4 compares the reflection coefficient and frequency. Figure 4 (a) shows that the preliminary blade antenna exhibits a limited operational bandwidth, and its reflection coefficient values ($S_{11}$) are not consistently below the −10 dBi threshold across the desired frequency range. This indicates poor impedance matching and reduced efficiency at several frequencies. By contrast, Figure 4 (b) shows the results for the optimized blade antenna design, where the $S_{11}$ curve demonstrates a much wider impedance bandwidth with values well below −10 dBi over a broad frequency range. This confirms that the optimization successfully improved the matching characteristics and enabled the antenna to support wideband operation. This improvement is primarily attributed to the introduction of slits on both the front and back of the blade radiator. These slits act as perturbations to the surface current paths, effectively generating additional resonances and enhancing multiband and broadband performance.

Figure 5 shows the current distributions for the preliminary and proposed blade antenna designs. Figure 5 (a) illustrates the

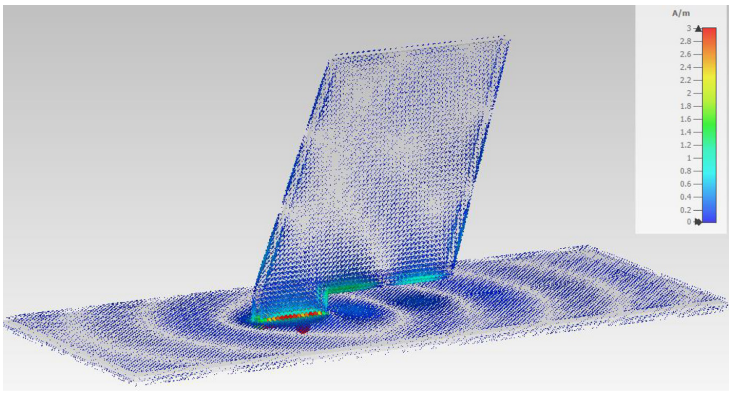

(a)

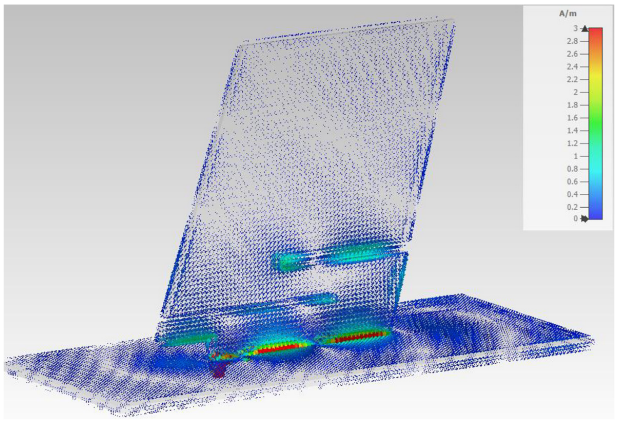

(b)

**Figure 5.** Surface current distribution at 1.03 GHz: (a) preliminary blade antenna and (b) optimized blade antenna

current distribution for the preliminary blade antenna design, where strong surface currents are concentrated near the feed region, with a relatively less effective distribution across the entire radiator. This limits the ability of the antenna to radiate efficiently at multiple frequency bands. In contrast, Figure 5 (b) demonstrates the optimized blade antenna, where the surface current is more evenly distributed across the blade structure, including regions around the introduced slits. The slits force the current to flow along multiple longer paths, creating additional resonant modes. This directly extends the bandwidth and improves the impedance matching.

Figure 6 shows the VSWR response of the optimized blade antenna over the frequency range of 0.4–1.1 GHz. The VSWR curve stays below the standard threshold of 2.0 for most of the operating band, which indicates good impedance matching between the antenna and the feed line. This ensures that minimal power is reflected toward the source, thereby improving radiation efficiency. At approximately 0.6 GHz and 0.9 GHz, the VSWR approaches its lowest points, demonstrating strong resonance and excellent matching at these frequencies. Although the curve slightly exceeds 2.0 in some regions, the majority of the band of interest remains within acceptable limits, confirming that the antenna is capable of supporting wideband operation.

The improved VSWR performance results from the optimized blade geometry, particularly the slit modifications, which introduce multiple current paths and resonant modes. This effectively broadens the bandwidth and enhances the suitability of the antenna for applications such as UHF SATCOM (400–500 MHz), TCAS/ADS-B (1030–1090 MHz), and UAV communication links.

Figure 7 illustrates the simulated 1D (E-plane cut) and 3D radiation patterns of the optimized blade antenna at the four frequency points. At the lower frequencies 0.43 and 0.50 GHz, the antenna demonstrates wide coverage with a more toroidal radiation pattern at the elevation plane, which is characteristic of monopole-like behavior, and is omnidirectional primarily in the azimuth plane. While at higher frequencies 1.03 and 1.09 GHz, the radiation becomes slightly more directive in some side directions with stronger main lobes. At these two frequencies, the peak gain is not located along the boresight ($\theta = 0°$)

**Table 1.** *Overall performance of the optimized blade antenna design*

| **Frequency point (GHz)** | **0.43** | **0.50** | **1.03** | **1.09** |
|---|---|---|---|---|
| Peak gain (dBi) | 7.753 | 7.363 | 8.282 | 8.197 |
| VSWR | 1.75 | 1.42 | 1.55 | 1.74 |
| Reflection coefficient ($S_{11}$) | −11.26 | −15.14 | −13.38 | −11.41 |

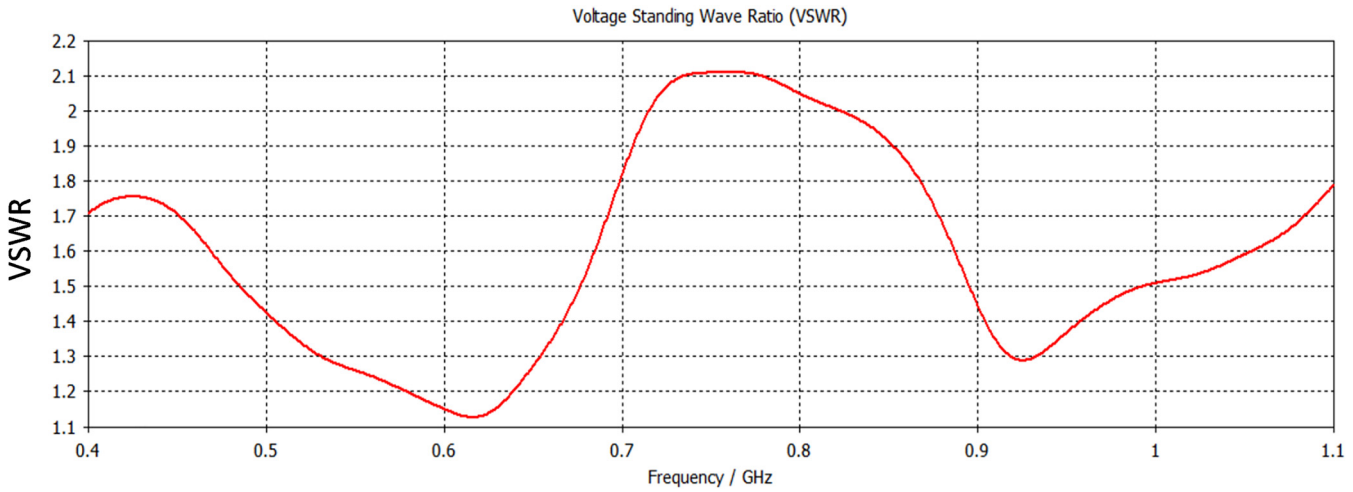


**Figure 6.** VSWR of the optimized blade antenna

but is slightly shifted (~25°–30° off-axis). This does not affect the ADS-B/TCAS performance, because these systems require toroidal or hemispherical coverage and do not focus on zenith gain. For the UHF SATCOM (400–500 MHz), the radiation remains closer to the boresight, ensuring reliable satellite link connectivity.

Table 1 summarizes the performance of the proposed blade antenna at the four frequency points: 0.43, 0.50, 1.03, and 1.09 GHz. The gain varies between 7.363 dBi and 8.282 dBi, with the highest values recorded at 1.03 GHz and 1.09 GHz. However, the radiation patterns in Figure 7 show that at these higher frequencies, the peak gain does not occur along the boresight, but instead shifts toward the side lobes, indicating that the antenna radiates more strongly in the off-axis directions. This is consistent with the slight asymmetry observed in the 3D radiation plots. The VSWR values remain below 2 across all frequencies, with the best impedance matching at 0.50 GHz (1.42), while the reflection coefficients are better than –10 dBi in all cases, reaching –15.14 dBi at 0.50 GHz.

Table 2 compares the proposed blade antenna with several representative designs reported in the literature. The existing designs by Belen et al.[9], Sairam et al.[10], and Saaquib et al.[11] generally prioritize either wideband behavior or specific aerospace applications, but they also exhibit notable limitations in gain, size, or functional coverage. For example, Sairam et al.[10] reported a compact fiber-reinforced polymer radome operating between 0.5–2.0 GHz, but the measured gain remains relatively low (3–5 dBi), making it more suitable for air-core EW and broadband systems than long-range UHF SATCOM. Similarly, the composite trapezoidal design by Belen et al.[9] covers 600–900 MHz with moderate gain (4.5–6.2 dBi) but lacks the operational bandwidth needed for simultaneous UHF SATCOM and ADS-B/TCAS support. The notched aluminum blade by Saaquib et al.[11] achieves good performance in the 835–962 MHz region; however, its gain (4.73–6.05 dBi) remains lower than that of the

**Table 2.** *Key performance metrics of comparison methods*

| Reference | Frequency range | Gain (dBi) | Bandwidth | Physical size | Applications |
|---|---|---|---|---|---|
| Belen et al., 2018 | 600–3000 MHz | 4.5–6.2 dBi (measured) | Ultra-wide (~150%) | Printed trapezoidal blade, multi-slot geometry | Very wideband UHF blade antenna |
| Sairam et al., 2018 | 0.5–2.0 GHz | 3–6 dBi (measured) | Very wide (~150%) | ~60 ×60 ×35 mm radiator (on 1.2 m ground plane) | Air-core coil, fiber-reinforced polymer radome, airborne electronic warfare applications |
| Saaquib et al., 2017 | 835–962 MHz | 4.73 dBi (simulated) / 6.05 dBi when aircraft-mounted | ~14% (928 MHz center) | 0.4 mm aluminum sheet blade (SolidWorks + CST design) | Notched blade with parasitic element |
| This study | 400–1100 MHz | 7.36–8.28 dBi | >60% | 400 ×850 mm ground plane; 490 mm height | Covers both UHF SATCOM (400–500 MHz) + ADS-B/TCAS (1030–1090 MHz) |

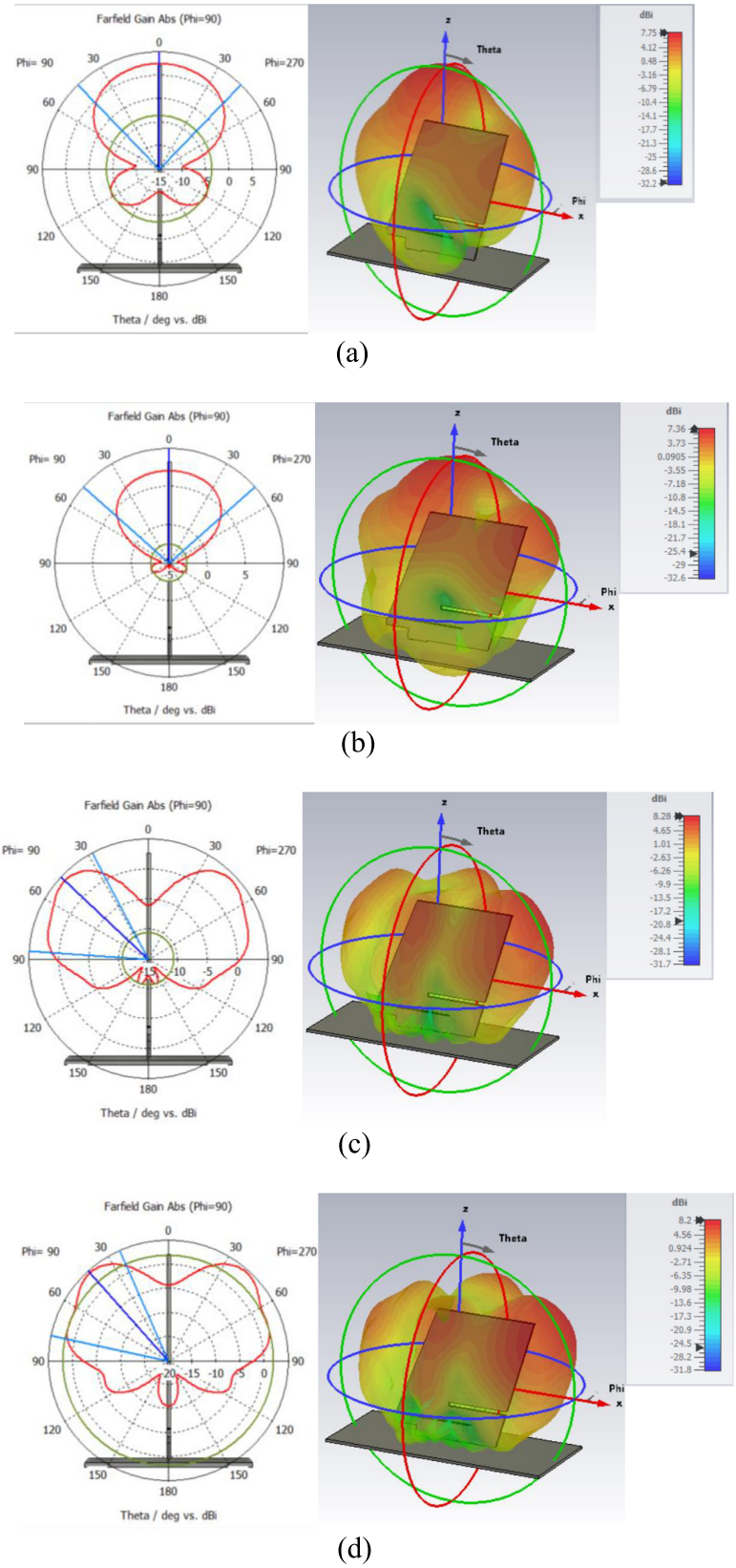


**Figure 7.** Radiation pattern as a (left) 1D E-plane cut and (right) 3D view of the optimized blade antenna at (a) 0.43 GHz; (b) 0.50 GHz; (c) 1.03 GHz; and (d) 1.09 GHz

optimized design, and its effective bandwidth is still limited to a single communication service.

By contrast, the optimized blade antenna developed in this study demonstrates a substantially broader operational range (400–1100 MHz) while simultaneously providing higher peak gain values (7.36–8.28 dBi) across the operational band. This represents a significant improvement in both radiation efficiency and multiservice compatibility. Within a single compact structure (400 ×850 mm ground plane and 490 mm height), the antenna successfully covers two critical aviation communication bands: the UHF SATCOM band (400–500 MHz), which requires robust hemispherical coverage for satellite connectivity, and the ADS-B/TCAS band (1030–1090 MHz), which requires reliable broadcast and surveillance performance. The achieved bandwidth, which exceeds 60%, further highlights the capability of the antenna to support diverse airborne systems without requiring multiple antennas or a larger fuselage volume. Overall, the results in Table 2 show that the proposed design outperforms previous state-of-the-art antennas in terms of gain, bandwidth, and dual-band coverage, thereby offering a more efficient and integrated solution for modern aviation platforms.

## 4. CONCLUSIONS AND FUTURE WORK

This study demonstrated the feasibility of a compact wideband blade antenna designed to support essential aeronautical communication functions. Using CST Studio Suite 2024, the antenna was simulated to evaluate the gain, surface current, and efficiency performance over the full 400 MHz to 1.1 GHz range. The results showed that the peak gain ranges from 7.363 to 8.282 dBi across the operational band, indicating stable efficiency and strong current distribution, making this design a strong candidate for future aerospace communication systems.

As mentioned above, the simulation model assumes a PEC. However, the real-world implementation of the antenna relies on aerospace-grade materials whose electromagnetic behavior differs from that of an ideal PEC. Real metallic structures, such as aluminum alloys or copper-plated composites, exhibit finite conductivity and surface resistance, which introduce small but measurable ohmic losses. Ramos et al.[16] provide a detailed electromagnetic characterization of aerospace materials, showing that factors such as surface finish, conductivity, composite lay-up, resin type, and bonding interfaces influence the overall electromagnetic performance of real structures. Their results demonstrated that even highly conductive aerospace materials can experience variations in shielding effectiveness, surface currents, and EM depending on the material composition and assembly conditions. These findings highlight the importance of considering real material conductivity rather than relying solely on PEC assumptions.

Therefore, the PEC-based simulations reported in this work represent an upper bound on antenna performance. When practical aerospace-grade conductors are used, the realized gain is expected to decrease by only an approximate of 0.2–0.4 dBi, which remains well within typical modelling and fabrication tolerances. This small deviation confirms that the PEC-based simulation results are accurate and reliable for the design assessment presented in this study. By addressing the need for a unified antenna across multiple aviation bands, this study contributes a practical solution for reducing onboard component load and improving aerodynamic efficiency. The simplicity of the design, combined with its robust broadband characteristics, paves the way for real-world implementation on both civil and military aircraft platforms.

This antenna type is suitable for a wide range of airborne applications. For TCAS/ADS-B (1030–1090 MHz), its high gain and directional performance support long-range aircraft identification and avoidance systems. For UHF SATCOM (~400–500 MHz), the antenna offers sufficient bandwidth and toroidal radiation patterns, making it a viable choice for satellite uplinks and emergency beacons. Furthermore, for unmanned aerial vehicles and remotely piloted aircraft, the compact profile allows seamless integration into unmanned platforms without compromising stealth or aerodynamic efficiency. Further research can explore dual-port or tunable versions for dynamic frequency allocation, as well as integration with conformal fuselage structures for enhanced stealth in defense applications.

## AFFILIATIONS AND AUTHOR DETAILS


### Undergraduate Author

**Taqi Abdulkhaleg Albaiyat** – *Aerospace Engineering Department, King Fahd University of Petroleum & Minerals, Saudi Arabia;* 0009-0006-7859-8710
Email: s202038980@kfupm.edu.sa

### Corresponding Author

**Bazilah Binti Baharom** – *Research Mentor, Interdisciplinary Research Centre for Aviation and Space Exploration, King Fahd University of Petroleum & Minerals, Saudi Arabia;* 0000-0003-3193-6197
Email: bazilah.baharom@kfupm.edu.sa


## ACKNOWLEDGEMENTS

The authors acknowledge the support provided by the Interdisciplinary Research Center for Aviation and Space Exploration at the King Fahd University of Petroleum and Minerals. The corresponding author also extends his appreciation to his advisor for guidance throughout the RES 200 Independent Research course, particularly for assistance in understanding antenna operations in aviation and aircraft applications, conducting the literature review, and supporting the antenna design process.

## REFERENCES

(1) D. De and P. K. Sahu, "A novel approach towards the designing of an antenna for aircraft collision avoidance system," *Int. J. Electron. Commun. (AEÜ)*, vol. 71, pp. 53–71. (2017).

(2) S. D. Ilcev, "Airborne satellite navigation and other integrated antenna systems," in *Proc. Int. Conf. Electrical, Electronics, and Optimization Techniques (ICEEOT)*. (2016).

(3) A. V. SE, S. J and T. Kavitha, "Conformal Antenna for Aircraft Applications," *2023 7th International Conference on Computation System and Information Technology for Sustainable Solutions (CSITSS)*, Bangalore, India, pp. 1–7. (2023).

(4) N. V. Laxminarayen, G. Lokeshwaran, K.S. Murugan and Dr. P. Jothilakshmi, "Design of conformal antenna for aircraft applications," in *Proc. Int. Conf. Smart Structures and Systems (ICSSS)*. (2017).

(5) M. Pallavi, P. Kumar, T. Ali, S. B. Shenoy and L. Sharma, "Design and Analysis of Patch Antenna with T-Shape DGS for Aircraft Surveillance Applications," *2022 6th International Conference on Green Technology and Sustainable Development (GTSD)*, Nha Trang City, Vietnam, pp. 1157–1163. (2022).

(6) Z. Ma and X. Huang, "Design of a circularly polarized microstrip antenna for aircraft tracking based on BeiDou III compatible with multi-navigation system," *Micromachines*, vol. 14, no. 11, p. 2083. (2023).

(7) Ö. Dündar and M. F. Ateş, "Use of microstrip antennas in aerospace applications: L5 band satellite communication example," *Aerospace Research Letters*, vol. 3, no. 1, pp. 69–78. (2024).

(8) A. Pascawati et al., "Blade Antenna 2.4 GHz for Rocket Applications," *2021 International Conference on Computer System, Information Technology, and Electrical Engineering (COSITE)*, Banda Aceh, Indonesia, pp. 204–208. (2021).

(9) A. Belen, H. P. Partal, S. Ördek and M. A. Belen, "Blade antenna design for UHF applications," *2018 26th Signal Processing and Communications Applications Conference (SIU)*, Izmir, Turkey, pp. 1–4. (2018).

(10) C. Sairam, T. Khumanthem, S. Ahirwar and S. Singh, "Broadband blade antenna for airborne applications," *2011 Annual IEEE India Conference*, Hyderabad, India, pp. 1–4. (2011).

(11) N. Saaquib, T. Sarker, N. Rahman, L. E. Khan and P. K. Saha, "Design and development of a wide band monopole blade antenna for aircraft navigation and communication," *2017 6th International Conference on Informatics, Electronics and Vision & 2017 7th International Symposium in Computational Medical and Health Technology (ICIEV-ISCMHT)*, Himeji, Japan, pp. 1–5. (2017).

(12) Silva, W.F., Bianchi, I., & Santos, T.P, "Design of a blade antenna embedded in low-cost dielectric substrate," *J. Microwaves, Optoelectronics and Electromagnetic Applications*, vol. 16, pp. 180193. (2017).

(13) M. Pallavi et al., "A review on gain enhancement techniques for vertically polarized mid-air collision avoidance antenna for airborne applications," *IEEE Access*, vol. 9, pp. 30761–30774. (2021).

(14) D. De and N. Chattoraj, "A review: Theoretical analysis of TCAS antenna," in *Proc. IEEE Int. Conf. Green Computing, Communication and Electrical Engineering (ICGCCEE)*. (2014).

(15) H. Li, W. Kinsner, Y. Wang, B. Palma and A. Tay, "Airborne Radar Based Collision Detection and Avoidance System for Unmanned Aircraft Systems in a Varying Environment," *2021 IEEE International Conference on Wireless for Space and Extreme Environments (WiSEE)*, Cleveland, OH, USA, pp. 43–48. (2021).

(16) Ramos. D, Cidrás. J, Plaza. B, Moravec. C, de la Torre. A, Frövel. M.R.K, Poyatos. D, " Novel Electromagnetic Characterization Methods for New Materials and Structures in Aerospace Platforms", *Materials*, vol. *15*, 5128. (2022).